Journal of Contaminant Hydrology, 12 (1993) 227–243
Elsevier Science Publishers B.V., Amsterdam

Mixing cell models for nonlinear equilibrium single species adsorption and transport

K. Bajracharya and D.A. Barry
Centre for Water Research, University of Western Australia, Nedlands, W.A. 6009, Australia

(Received May 20, 1992; revised and accepted November 9, 1992)

ABSTRACT

Bajracharya, K. and Barry, D.A., 1993. Mixing cell models for nonlinear equilibrium single species adsorption and transport. J. Contam. Hydrol., 12: 227–243.

A simple improved mixing cell model is shown to be more accurate than the standard mixing cell model when used to solve solute transport problems with a nonlinear adsorption isotherm included. The solution obtained from the improved model is found to agree closely with that calculated using a Crank–Nicolson scheme, and an exact analytical solution for solute transport subject to a nonlinear solute adsorption isotherm. Application of the improved mixing cell model was demonstrated by application to experimental data from a laboratory Ca–K exchange experiment in which a solution containing Ca was passed through a column filled with K-saturated soil. The model was used in conjunction with the experimentally determined nonlinear adsorption isotherm to predict the experimental breakthrough data. The data and the predictions agreed reasonably well, indicating that the equilibrium assumption is reasonable. However, it is suggested that an appropriate isotherm is necessary to describe well the concentration history curve.

1. INTRODUCTION

Various industrial processes, mining, and other anthropogenic activities create by-products which are capable of degrading the environment. High-profile debate over the desirability of industrial proposals vis-à-vis the concomitant disposal problems is commonplace. Solute with a high migration rate through the soil profile may endanger groundwater supplies while a low migration rate may result in accumulation of contaminants in the near-surface soil layers, and therefore have detrimental effects on terrestrial biota. The ability to control the fate of contaminants in the soil environment or, rather,

Correspondence to: K. Bajracharya, Centre for Water Research, University of Western Australia, Nedlands, W.A. 6009, Australia.

0169-7729/93/$06.00

NOTATION

List of symbols used in this paper

Symbol	Description	Dimension
a_i	constants defined in eq. 22 (i = 1,2,3)	[L T^{-1}]
A_i	arbitrary constants (i = 1,2,3)	
C_r	Courant number, $V\Delta t/\Delta z$	
C	normalised liquid-phase concentration	
C_0	normalised influent concentration	
C^*	boundary layer corrected normalised liquid-phase concentration	
D_{num}	numerical dispersion coefficient	[L^2 T^{-1}]
D_s	dispersion coefficient	[L^2 T^{-1}]
$D(\theta)$	soil-water diffusivity	[L^2 T^{-1}]
D_0	value of the soil-water diffusivity at the residual water content	[L^2 T^{-1}]
g	function defined by eq. 29	
G	amplification factor	
k_i	constants defined in eqs. 23 and 24 (i = 1,...,6)	
$K(\theta)$	hydraulic conductivity	[L T^{-1}]
K_s	value of the hydraulic conductivity at the saturated water content	[L T^{-1}]
L	length of column	[L]
P	Péclet number, VL/D_s	
R	retardation factor	
S	normalised solid-phase concentration	
S^*	boundary layer corrected normalised solid-phase concentration	
t	time	[T]
u	total normalised solute concentration	
u^*	boundary layer corrected total normalised solute concentration	
V	mean pore-water velocity	[L T^{-1}]
z	distance below surface	[L]
β	variable defined by eq. 20	
θ	moisture content	
θ_i	initial moisture content	
φ	Fourier mode	
μ	variable defined by eq. 31	
ν	fitting parameter in eq. 22	
ψ	moisture tension	[L]
ω	weighting factor	
Δt	time step	[T]
Δz	spatial step	[L]

contaminant mobility, relies on understanding the basic mechanisms causing attenuation of contaminants in general.

Presently, there is a wide variety of models available for predicting solute movement. Thorough discussions of the various numerical and analytical models and their attributes have been given recently by Mangold and Tsang (1991) and Barry (1992). Barry (1992) discusses the significant computational requirements of general purpose flow and transport codes. For routine use, simple models which are easy to code, efficient to compute, and which can be

linked with chemical speciation models, are valuable tools. Such an approach is embodied in mixing cell models.

Many papers (e.g., Schweich and Sardin, 1981; Schulz and Reardon, 1983; Schweich et al., 1983; Van Ommen, 1985; Rao and Hathaway, 1989; Dudley et al., 1991) have appeared on the use of the simple mixing cell models but none of them describe details of the error analysis. Such an analysis is carried out below with the surprising result that the inclusion of an adsorption isotherm in the transport equation reduces the accuracy of the model. We present an improved mixing cell model that does not suffer from this defect. The main purpose of this paper is to show the use of the improved mixing cell model as applied to reactive solute transport. This is done by coupling various typical adsorption isotherms with the solute transport equation and comparing the predictions of the mixing cell model with those from a Crank–Nicolson scheme, and analytical solutions where possible. Data from the well controlled K–Ca exchange experiment of Schweich et al. (1983) are used to illustrate the practical applicability of the improved mixing cell model.

2. THEORY

2.1. Transport with equilibrium reaction

The advection–dispersion solute transport equation with reaction is given by (e.g., Yortsos, 1987):

$$\frac{\partial u}{\partial t} = D_s \frac{\partial^2 C}{\partial z^2} - V \frac{\partial C}{\partial z} \tag{1}$$

where

$$u = C + S(C) \tag{2}$$

In eq. 2, u is the total solute concentration in the soil (symbols are collected in the Notation). The adsorbed phase solute concentration, S, is assumed to be given as an equivalent fluid-phase concentration.

2.1.1. Boundary conditions. The boundary conditions at both ends of the column can affect the breakthrough curve. However, in many cases only the boundary condition at the column entrance affects the profile within the column to any extent (Parlange and Starr, 1975). An exhaustive discussion of boundary conditions is given by Barry and Sposito (1988). Two sets of boundary conditions are considered in particular. One set commonly applied at the entrance and exit, respectively, consists of:

$$C(0,t) = C_0 \tag{3}$$

and

$$\left.\frac{\partial C}{\partial z}\right|_{z\to\infty} = 0 \tag{4a}$$

Condition (3)is usually applied in the case of flux concentrations (Kreft and Zuber, 1978). This condition implies continuity of concentration at the surface. Condition (4a) simply states that the solute concentration remains bounded for the semi-infinite column. The second set of boundary conditions is described below.

In the case of resident concentrations, the boundary condition at the entrance is given by (Danckwerts, 1953):

$$VC(0,t) - D_s\frac{\partial C(0,t)}{\partial z} = VC_0 \tag{5}$$

At the exit, the condition imposed is:

$$\left.\frac{\partial C}{\partial z}\right|_{z\to L} = 0 \tag{4b}$$

which simply assumes the continuity of solute across the column exit. Parlange and Starr (1975, 1978) have shown that, as long as $P > 4$, breakthrough curves calculated using eqs. 1, 4b and 5 (at $z = L$) can be very closely approximated by the solution found using eqs. 1, 3 and 4a. We will make use of this result while comparing an exact solution with the improved mixing cell model.

2.1.2. Initial conditions. The initial normalised solute concentration in both the solid and liquid phases is:

$$C(z,0) = C_i \tag{6a}$$

$$S(z,0) = S_i \tag{6b}$$

The right-hand sides of eqs. 6a and 6b can assume zero or non-zero values, or vary with position, z.

2.2. Mixing cell models

To derive the mixing cell models, the dispersive term in eq. 1 is neglected and the advective transport equation given by:

$$\frac{\partial[C+S(C)]}{\partial t} = -V\frac{\partial C}{\partial z} \tag{7}$$

is solved. Mixing cell models are explicit finite-difference representations of eq. 7. The temporal derivative is written as a forward difference and the advective component is approximated by a backward difference that is a

weighted average of two time levels, i.e.:

$$\frac{C(i,j+1)-C(i,j)}{\Delta t}+\frac{S(i,j+1)-S(i,j)}{\Delta t} =$$

$$-V\left[\omega\left(\frac{C(i,j+1)-C(i-1,j+1)}{\Delta z}\right)+(1-\omega)\left(\frac{C(i,j)-C(i-1,j)}{\Delta z}\right)\right] \tag{8a}$$

where $C(z,t) = C(i\Delta z, j\Delta t) = C(i,j)$ and $0 \leqslant \omega \leqslant 1$.

After some simplification, the general scheme is obtained as:

$$(1+\omega C_r)C(i,j+1)+S(i,j+1) = [C(i,j)+S(i,j)]$$

$$+C_r[\omega C(i-1,j+1)+(1-\omega)\{C(i-1,j)-C(i,j)\}] \tag{8b}$$

where

$$C_r = \frac{V\Delta t}{\Delta z} \tag{9}$$

is the Courant number. The solid-phase concentration is given by:

$$S(i,j+1) = f[C(i,j+1)] \tag{10}$$

and hence eq. 8b reduces to a single (usually nonlinear) equation in $C(i,j+1)$ which can be easily solved numerically. When $\omega = 0$, the scheme (8b) becomes the standard mixing cell model used by Van Ommen (1985). Eq. 8b reduces to the scheme used by Dudley et al. (1991) when ω takes the value 1. The scheme becomes the improved mixing cell model when ω assumes the value $\frac{1}{2}$, the case considered in detail in this study.

2.2.1. Consistency analysis. Using Taylor series expansions about $C(i,j)$ in eq. 8a, we find:

$$\frac{\partial u}{\partial t}+\frac{\Delta t}{2}\frac{\partial^2 u}{\partial t^2} = -V\frac{\partial C}{\partial z}+\frac{V\Delta z}{2}\frac{\partial^2 C}{\partial z^2}-\omega V\Delta t\frac{\partial^2 C}{\partial t\partial z}+O(\Delta z\Delta t,\Delta z^2,\Delta t^2) \tag{11}$$

Differentiating eq. 11 with respect to t and dropping terms higher than first order we have:

$$\frac{\partial^2 u}{\partial t^2} = -V\frac{\partial}{\partial z}\left(\frac{\partial C}{\partial t}\right)+O(\Delta z,\Delta t) \tag{12}$$

Differentiating eq. 11 again but with respect to z and noting eq. 2, we get:

$$\frac{\partial}{\partial z}\left(\frac{\partial C}{\partial t}\right) = -V\frac{\partial^2 C}{\partial z^2}-\frac{\partial}{\partial z}\left(\frac{\partial S}{\partial t}\right)+O(\Delta z,\Delta t) \tag{13}$$

The combination of eqs. 11, 12 and 13 gives:

$$\frac{\partial u}{\partial t} = \frac{V\Delta z}{2}[1 - 2C_r(\tfrac{1}{2}-\omega)]\frac{\partial^2 C}{\partial z^2} - V\frac{\partial C}{\partial z} - V\Delta t(\tfrac{1}{2}-\omega)\frac{\partial^2 S}{\partial z \partial t} + O(\Delta z\Delta t, \Delta z^2, \Delta t^2) \tag{14a}$$

If $S(C) = 0$ then the scheme (8b) has a truncation error of $O(\Delta z^2, \Delta t^2)$. Since adsorption is to be considered, the error of scheme (8b) is $O(\Delta z^2, \Delta t)$ if $\omega \neq \frac{1}{2}$. For the special case of a linear isotherm, $u = RC$, the equivalent equation to eq. 14a is:

$$R\frac{\partial C}{\partial t} = \frac{V\Delta z}{2}[1 - 2C_r(\tfrac{1}{2}-\omega)]\frac{\partial^2 C}{\partial z^2} - V\frac{\partial C}{\partial z} + O(\Delta z\Delta t, \Delta z^2, \Delta t^2) \tag{14b}$$

Thus, for $S(C) = 0$ or $S(C) = (R-1)C$, the mixing cell models are always accurate to second order, for any choice of ω. This method will introduce a numerical dispersion coefficient, D_{num}, given by:

$$D_{num} = \frac{V\Delta z}{2}[1 - 2C_r(\tfrac{1}{2}-\omega)] \tag{15}$$

When the advective–dispersive transport equation (1) is to be solved using the mixing cell model, i.e. eq. 8b, the relation $D_s = D_{num}$ is imposed. This fixes the relationship between optimal step lengths and time intervals. From eq. 15, it is evident that we must have $\Delta z >$, $=$, or $< 2D_s/V$ according to whether $\omega = 0$, $\frac{1}{2}$, or 1, respectively.

Peaceman (1977) considers a hyperbolic equation mathematically identical to eq. 7. However, his analysis is based on the linearised version of eq. 7, i.e. he considers S to be linear in C as we did to arrive at eq. 14b. For that case, as we have seen, choosing ω is inconsequential insofar as the truncation error is always $O(\Delta z^2, \Delta t^2)$, and provided that the numerical dispersion term is equated to D_s. The present analysis, by contrast, reveals the intriguing result that $\omega = \frac{1}{2}$ maintains the truncation error regardless of whether S is a linear or nonlinear algebraic function of C.

2.2.2. Stability analysis. The von Neumann stability method (Noye, 1982) is used to check that eq. 8b is stable. The method relies on linearity of the scheme investigated, and so cannot be applied for nonlinear adsorption isotherms. Upon applying the method to the error equation, without considering the solid-phase concentration, we see that the error amplification factor G is given by:

$$G = \frac{1+(1-\omega)C_r(1-\cos\varphi) - \sqrt{-1}(1-\omega)C_r\sin\varphi}{1+\omega C_r(1-\cos\varphi) + \sqrt{-1}\omega C_r\sin\varphi} \tag{16}$$

For stability, we must have $|G|^2 \leqslant 1$ and so eq. 16 yields:

$$1 - C_r(1-2\omega) \geqslant 0 \tag{17}$$

which is always true for $\omega \geq \frac{1}{2}$ and hence the scheme is unconditionally stable for those schemes with ω satisfying this condition. For $\omega = 0$, the scheme is stable for $C_r \leq 1$. When a linear isotherm is considered this scheme is stable for $C_r \leq R$. Of course, condition (17) only provides an indication of the stability behaviour of the scheme. However, the scheme was checked numerically using different nonlinear isotherms. In all cases the results were found to agree with condition (17).

2.2.3. Boundary layer correction. The effect of eq. 4b is to increase solute concentration in the profile in the region $z \approx L$ (Parlange and Starr, 1978). For $P > 4$, corrections can be applied to the solutions obtained for semi-infinite systems to approximate the solution for a finite length profile. The procedure to obtain such a correction is given by Barry et al. (1986). A similar approach is used to obtain the following relation:

$$C^*(z,t) = C(z,t) - \frac{2D_s \exp\left(\frac{V\beta(z-L)}{2D_s}\right)}{V\beta} \left.\frac{\partial C}{\partial z}\right|_{z=L} \tag{18}$$

where $C(z,t)$ is the solution obtained for a semi-infinite column and:

$$u^* = C^* + S^*(C^*) \tag{19}$$

The parameter β in eq. 18 is given by:

$$\beta = 1 + \left[1 - \frac{4D_s}{V}\left\{\frac{\partial}{\partial z}\left(\ln \frac{\partial C}{\partial z}\right)\right\}_{z=L}\right]^{1/2} \tag{20}$$

Below, the correction (18) is applied to an exact solution of eqs. 1, 4a and 5, with the nonlinear isotherm given by eq. 22, to obtain the approximate solution for a finite column.

3. COMPARISON WITH OTHER SOLUTIONS

The mixing cell models are first compared by considering a linear isotherm. The improved mixing cell model is then compared with an exact nonlinear solution with the boundary layer correction. The improved mixing cell model is also compared with a more accurate Crank–Nicolson numerical solution considering two types of nonlinear isotherms to show the effect of the nature of isotherm on the shape of the breakthrough curve. This effect is also apparent in Section 4, where laboratory data are simulated.

3.1. Linear isotherm

The mixing cell models are compared with the exact analytical solution in which a linear isotherm, $S = (R-1)C$, is assumed. The exact analytical

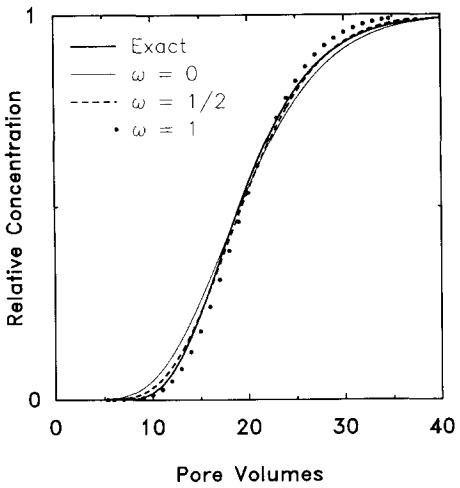

Fig. 1. Comparison of standard ($\omega = 0$) mixing cell model ($V\Delta z/D_s = 2.5$, *thin line*), improved ($\omega = \frac{1}{2}$) mixing cell model ($V\Delta z/D_s = 2$, *dashes*), fully implicit ($\omega = 1$) mixing cell model ($V\Delta z/D_s = 1.43$, *solid circles*) and exact (*thick line*) solutions for a linear isotherm ($R = 20$, $P = 20$).

solution for eqs. 1, 3 and 4a for this isotherm is given by (e.g., van Genuchten and Alves, 1982):

$$\frac{C(z,t)}{C_0} = \frac{1}{2}\left[\operatorname{erfc}\left(\frac{Rz - Vt}{\sqrt{4D_s Rt}}\right) + \exp\left(\frac{Vz}{D_s}\right)\operatorname{erfc}\left(\frac{Rz + Vt}{\sqrt{4D_s Rt}}\right)\right] \tag{21}$$

The simulations of breakthrough curves have been done for $R = 20$ and $P = 20$. The retardation factor is relatively large, and simulates a strongly adsorbed solute. It is evident from Fig. 1 that the improved mixing cell solution ($\omega = \frac{1}{2}$) is more accurate than the standard mixing cell ($\omega = 0$) and the fully implicit mixing cell solution ($\omega = 1$). We observe (simulations not shown) that for $\omega = 0$, as the spatial step increases the error increases. On the other hand, for $\omega = 1$, increasing the spatial step tends to improve the solution. Because C_r disappears from condition (15) for $\omega = \frac{1}{2}$, Δt can be chosen independently, and so the improved mixing cell allows the use of a greater time step than the other mixing cell models while maintaining greater accuracy. Note that for $\omega \neq \frac{1}{2}$, condition (15) was used to fix the spatial and temporal steps in the simulation of breakthrough curves by the mixing cell models. The simulations done in the following are all by the improved mixing cell model.

3.2. Comparison with an exact solution using a nonlinear isotherm

Barry and Sander (1991) have given an exact solution for a nonlinear isotherm derived from the correspondence of the infiltration equation with the

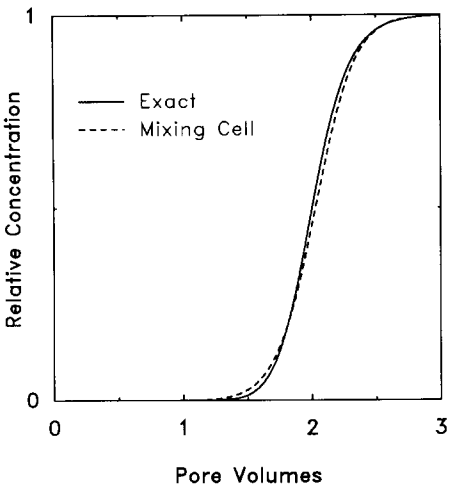

Fig. 2. Comparison of improved mixing cell model and exact solution with boundary layer correction for the nonlinear isotherm eq. 22 shown in Fig. 5 ($P = 35$).

solute transport equation. Their isotherm is of the form:

$$S(C) = \frac{\sum_{i=0}^{2} a_i C^i}{K_s A_2 (v - 1) - A_2 A_3 v - a_2 C} \tag{22}$$

It should be noted that their solution is for a semi-infinite column and satisfies boundary condition (5). Fig. 2 shows the exact solution with boundary layer correction (18) and the solution using improved mixing cell model with the above isotherm. The entrance boundary condition used in improved mixing cell is eq. 3. We observe that the mixing cell model prediction is quite close to the exact solution. The Crank–Nicolson solution (see below) with boundary condition (5) produces an identical fit with the exact solution and is not shown in the figure.

3.3. Comparison with a Crank–Nicolson scheme

The reactive solute transport equation (1) is also solved by the Crank–Nicolson method which has an error of $O(\Delta z^2, \Delta t^2)$. This is a common way to solve eq. 2 numerically. Barry et al. (1983, 1987) solve eq. 1 for an isotherm, $S(C)$, that is linear in C, but explicitly nonlinear in z and t. Except for this difference, the problem solved is identical to the case of interest here and so the latter is solved by the same approach.

Sposito (1989) categorises four classes of adsorption isotherm observed commonly in soil research. Two different types of isotherm are considered to indicate the effect on the shape of the breakthrough curve, an S-curve and a

Freundlich isotherm. Barry (1992) has given an S-shaped isotherm which is of the form:

$$S = k_4[1-\{1+(k_2C)^{k_1}\}^{k_3}] \tag{23}$$

The Freundlich isotherm is:

$$S = k_5 C^{k_6} \tag{24}$$

Fig. 3a shows the S-curve and Freundlich isotherms used for the purpose of comparison (constants used to calculate the isotherms are given in the figure caption). Fig. 3b shows the breakthrough curves for S-curve isotherm as simulated by Crank–Nicolson scheme and the improved mixing cell model. In Fig. 3c we show the breakthrough curves for Freundlich isotherm as simulated by the Crank–Nicolson scheme and the improved mixing cell model. In each case the mixing cell model prediction is very close to the Crank–Nicolson scheme. Also mixing cell solution was observed to be much faster than the Crank–Nicolson scheme. Note that the boundary conditions used in Crank–Nicolson scheme are identical with those of the improved mixing cell model.

It is clear from Fig. 3b and c that the type of isotherm has a profound effect on the shape of the breakthrough curve. At lower concentrations, the S-curve produces little adsorption and, as a result, the concentration rise is earlier. In case of the Freundlich isotherm, adsorption is quite high at lower concentrations as compared with the S-curve, resulting in a delayed rise in concentration. Also the isotherm slope, dS/dC, decreases with C for the Freundlich isotherm whereas, for the S-curve, the slope initially increases with C, reaches a maximum and then decreases. In the latter case (Fig. 3b) the initial increase in slope has flattened the breakthrough curve and the decrease has sharpened it later. For an increasing slope, the breakthrough curve flattens or shows a tailing effect. The extent of flattening or sharpening is again dependent on the rate of increase or decrease in the slope, dS/dC.

4. COMPARISON WITH EXPERIMENTAL RESULTS

Results of Ca–K exchange during soil column miscible displacement experiments reported by Schweich et al. (1983) are considered here. The column was filled initially with K-saturated soil and was subjected to an influent solution containing Ca at a fixed normality under the condition of steady flow. They also carried out a miscible displacement experiment where Ca in the influent solution was exchanged on a Ca-saturated soil. The breakthrough curve from this experiment can be analysed as for a tracer displacement experiment.

The tracer data are reproduced in Fig. 4. The improved mixing cell model

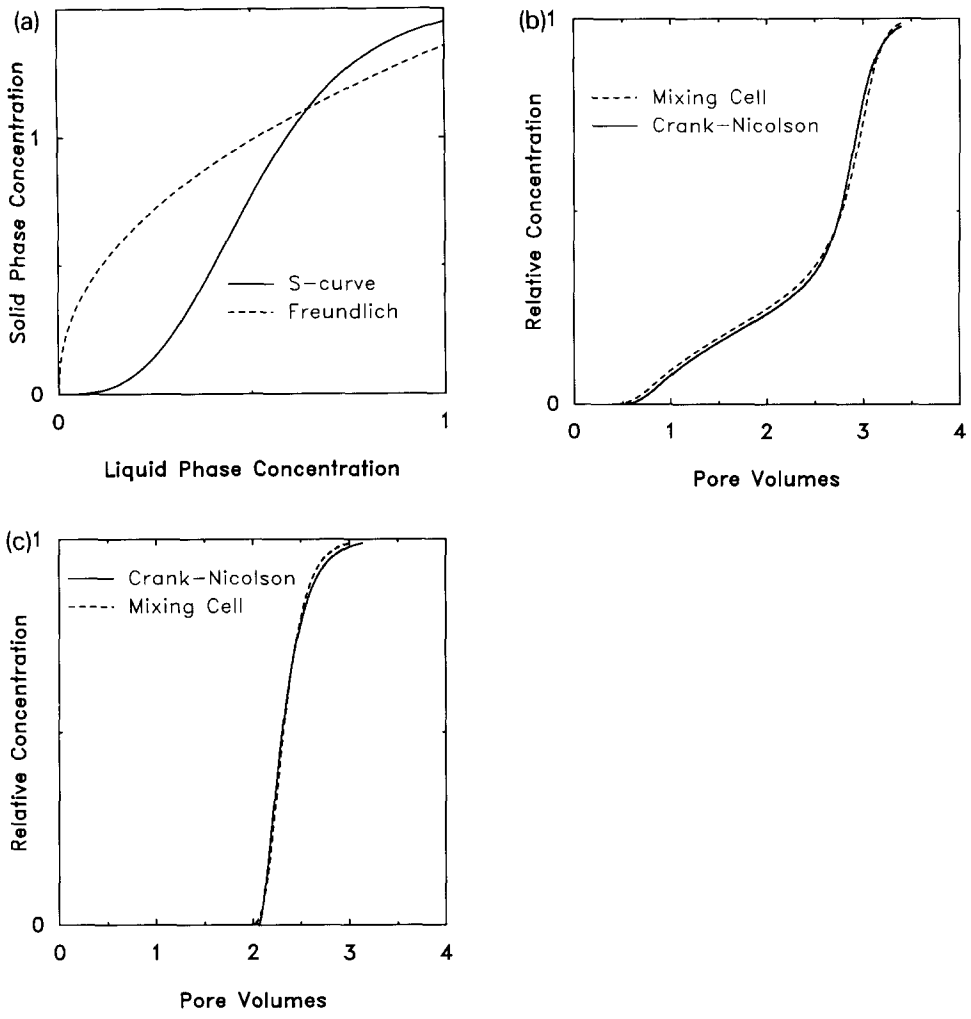

Fig. 3. a. S-curve isotherm ($k_1 = 3$, $k_2 = 1.5$, $k_3 = -2$, $k_4 = 1.5299$) and Freundlich isotherm ($k_5 = 1.3572$, $k_6 = 0.4560$).
b. Comparison of improved mixing cell model with Crank–Nicolson scheme for the S-curve shown in (a) ($P = 35$).
c. Comparison of improved mixing cell model with Crank–Nicolson scheme for the Freundlich isotherm shown in (a) ($P = 35$).

fits the data very well and is shown in the same figure. It is found that a good fit was obtained with $P = 35$. The analytical solution (eq. 21 with $R = 1$) produces a similarly good fit for the same Péclet number (not shown in the figure). Note that $P >> 4$ so that the breakthrough curves calculated at the column exit from the solution of eq. 1, with eqs. 3 and 4a as the entrance and exit boundary conditions, approximates the breakthrough curves calculated

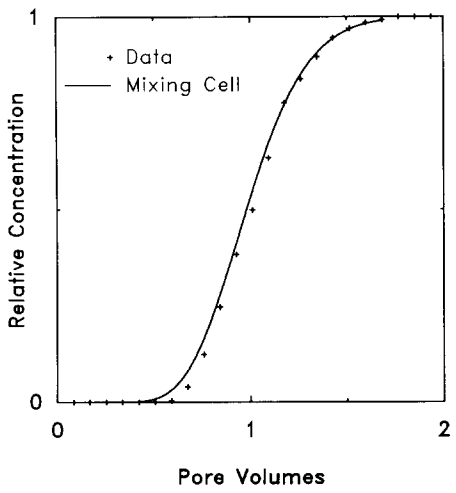

Fig. 4. Improved mixing cell model simulation of the tracer data of Schweich et al. (1983) for $P = 35$.

from the solution of eq. 1 for a finite column (with eq. 5 as the entrance boundary condition and eq. 4b applying at the column exit).

The experimental isotherm used by Schweich et al. (1983) is graphically shown in Fig. 5. The data from their batch experiments are also shown in the figure. Note that, in the figure, the solid-phase concentration has been converted to the normalised solution-phase concentration scale. The

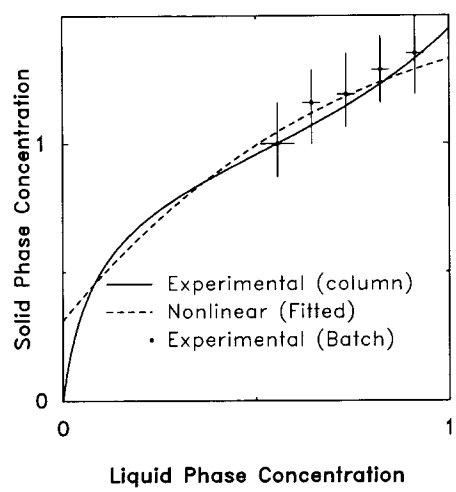

Fig. 5. Experimental column isotherm, fitted nonlinear isotherm equation (24) ($a_1 = -0.2083$, $a_2 = -1.3329$, $a_3 = 0.2775$, $A_1 = 0.2594$, $A_2 = 0.3295$, $A_3 = 0.3124$, $K_s = 2.1257$, $v = 0.0473$) and experimental batch data of Schweich et al. (1983). (The vertical and horizontal segments for each point indicate the error range of the measurement.)

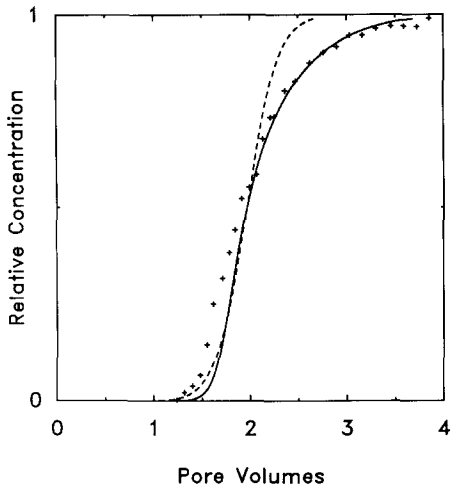

Fig. 6. Improved mixing cell model simulations of breakthrough data (+) of Schweich et al. (1983) using experimental isotherm (*line*) and fitted nonlinear isotherm (*dashes*) for $P = 35$ (isotherms shown in Fig. 5).

isotherm, eq. 22, was fitted to the experimental isotherm. This fit is also shown in the same figure.

Fig. 6 shows the predictions of the improved mixing cell model for the two isotherms shown in Fig. 5 and the experimental data collected by Schweich et al. (1983, fig. 4). The prediction using the fitted isotherm (eq. 22) for $P = 35$, does not replicate the spreading of the breakthrough curve. It should be borne in mind that the nature of the isotherm affects the shape of the breakthrough curve as was shown in Fig. 3b and c. The simulation of the breakthrough curve for the experimental isotherm using mixing cell model predicts the data quite well. However, the lower portion is still not well described.

5. DISCUSSION

In a previous study (Barry et al., 1991), the isotherm equation (22) was fitted to the experimental isotherm and the breakthrough curve obtained by exact solution was compared with the breakthrough data. Their result (dashed curve in Fig. 6) has been reproduced making use of the mixing cell model. Clearly, the results do not agree well with the experimental data for $P = 35$. The main difference is that the experimental data show more enhanced spreading of the breakthrough curve. It is seen that when the experimental isotherm is used, the same mixing cell scheme yields a reasonably good fit. The results suggest that a local equilibrium model is a valid assumption for most of the adsorption process taking place. The simulation by the Crank–Nicolson solution (not shown in Fig. 6) also gives the same results with the same

experimental isotherm. Therefore, the Ca–K ion exchange, as modelled by the experimental isotherm, produces the enhanced spreading of the upper portion of the breakthrough curve. Clearly, the type of isotherm is very important in determining the shape of the breakthrough curve. In Fig. 5, the slope dS/dC of the fitted isotherm (eq. 22) is decreasing with C whereas in the experimental isotherm, the slope first decreases and then increases with C. It is likely that this increase in slope dS/dC is responsible for the tailing of the breakthrough curve.

We observe in Fig. 6 that the breakthrough curve obtained using the experimental isotherm of Schweich et al. (1983) fails to predict the lower limb of the breakthrough curve. This shows that the isotherm used is still not an appropriate one at lower concentrations. The early rise initially in the experimental breakthrough curve (~ 1.5 pore volumes) is possibly due to lesser adsorption at lower concentrations than given by the experimental isotherm. In Fig. 5 we have included the experimental batch data of Schweich et al. (1983). A thorough comparison is hindered by the lack of data at lower concentrations. At higher concentrations, however, the isotherm is appropriate and hence the upper part of the breakthrough is well described. This example demonstrates again the importance of the isotherm in determining the shape of the breakthrough curve.

5.1. Mixing cell solution for Richards' equation

The improved mixing cell model can be used to solve the unsaturated flow equation (Richards, 1931):

$$\frac{\partial \theta}{\partial t} = \frac{\partial}{\partial z}\left(D(\theta)\frac{\partial \theta}{\partial z} - K(\theta) \right) \tag{25}$$

subject to the conditions:

$$\theta(z,0) = \theta_i \tag{26}$$

$$\theta(0,t) = \theta_0 \tag{27}$$

and

$$\left.\frac{\partial \theta(z,t)}{\partial z}\right|_{z \to \infty} = 0 \tag{28}$$

Physically, this models unsaturated fluid flow into a semi-infinite soil profile with an initial moisture content, θ_i, with $\theta = \theta_0$ at the soil surface. We transform eq. 25 using the Kirchhoff prescription:

$$g = \int_{\theta_i}^{\theta} D(\theta')\mathrm{d}\theta' \tag{29}$$

Eq. 25 becomes:

$$\frac{\partial\theta}{\partial t} = \frac{\partial^2 g}{\partial z^2} - \mu\frac{\partial g}{\partial z} \tag{30}$$

where

$$\mu = \frac{1}{D(\theta)}\frac{\mathrm{d}K(\theta)}{\mathrm{d}\theta} \tag{31}$$

Eq. 29 gives g uniquely in terms of θ and so, conversely, we have $\theta(g)$. For any $\theta(g)$, we can write:

$$\theta(g) = g + f(g) \tag{32}$$

in which case eq. 30 has the form of the solute transport model, eq. 1. The initial and boundary conditions used in the solution of eq. 30 can easily be determined from eqs. 26–28 and 32. If μ defined in eq. 31 is constant, then the mixing cell model presented in this paper can be used immediately to solve eq. 30. The condition of μ constant is not as restrictive as first appears. Parlange (1980), for example, uses μ constant near saturation to derive a formula for cumulative infiltration as a function of time. This assumption represents a limiting case of soil behaviour (Parlange, 1980). Eq. 31 states that this condition is assumed to hold for all θ, not just near saturation, and thus represents a particular soil type. Indeed, for μ constant, since:

$$D(\theta) = K(\theta)\frac{\mathrm{d}\psi}{\mathrm{d}\theta}$$

eq. 31 implies:

$$K(\psi) \propto \exp(\mu\psi) \tag{33}$$

Eq. 33 was first presented by Gardner (1958).

6. CONCLUSIONS

The main purpose of this paper was to show the use of a simple improved mixing cell model for predicting solute transport subject to a nonlinear equilibrium adsorption isotherm. It is found that the improved mixing cell model ($\omega = \frac{1}{2}$) is more accurate than the mixing cell models with ($\omega = 0, 1$) while involving a similar computational load. The scheme compares favourably in terms of accuracy with a corresponding Crank–Nicolson solution. Various applications of the mixing cell model showed that the shape of the breakthrough curve is affected by the nature of the adsorption isotherm. Finally, we showed that unsaturated flow in soils described by Gardner (1958) formulation of the unsaturated hydraulic conductivity can also be described by the mixing cell model.

ACKNOWLEDGMENTS

The authors acknowledge the support of the Australian Research Council.

REFERENCES

Barry, D.A., 1992. Modelling contaminant transport in the subsurface: Theory and computer programs. In: H. Ghadiri and C.W. Rose (Editors), Modelling Chemical Transport in Soil: Natural and Applied Contaminants. Lewis, Chelsea, MI, pp. 105–144.

Barry, D.A. and Sander, G.C., 1991. Exact solutions for water infiltration with an arbitrary surface flux or nonlinear solute adsorption. Water Resour. Res., 27(10): 2667–2680.

Barry, D.A. and Sposito, G., 1988. Application of the convection–dispersion model to solute transport in finite soil columns. Soil Sci. Soc. Am. J., 52(1): 3–9.

Barry, D.A., Starr, J.L., Parlange, J.-Y. and Braddock, R.D., 1983. Numerical analysis of the snow-plow effect. Soil Sci. Soc. Am. J., 47(5): 862–868.

Barry, D.A., Parlange, J.-Y. and Starr, J.L., 1986. Interpolation method for solving the transport equation in soil columns with irreversible kinetics. Soil Sci., 142(5): 296–307.

Barry, D.A., Parlange, J.-Y. and Starr, J.L., 1987. Numerical analysis of the precursor effect. Soil Sci., 143(5): 309–317.

Barry, D.A., Sander, G.C. and Phillips, I.R., 1991. Modelling solute transport, chemical adsorption and cation exchange. Int. Hydrol. Water Resour. Symp., Inst. Eng., Perth, W.A., Oct. 2–4, Inst. Eng. Aust., Prepr. Pap. (Natl. Conf. Ser.), 3: 913–918.

Danckwerts, P.V., 1953. Continuous flow systems — Distribution of residence times. Chem. Eng. Sci., 2: 1–13.

Dudley, L.M., Mclean, J.E., Furst, T.H. and Jurinak, J.J., 1991. Sorption of cadmium and copper from an acid mine waste extract by two calcareous soils: Column studies. Soil Sci., 151(2): 121–135.

Gardner, W.R., 1958. Some steady state solutions of the unsaturated moisture flow equation with application to evaporation from a water table. Soil Sci., 85(4): 228–232.

Kreft, A. and Zuber, A., 1978. On the physical meaning of the dispersion equation and its solutions for different initial and boundary conditions. Chem. Eng. Sci., 33: 1471–1480.

Mangold, D.C. and Tsang, C.-F., 1991. A summary of subsurface hydrological and hydro-chemical models. Rev. Geophys., 29(1): 51–79.

Noye, J., 1982. Numerical solutions of partial differential equations. In: Proceedings of the 1981 Conference on the Numerical Solutions of Partial Differential Equations held at Queen's College, Melbourne University, Australia. North-Holland Publishing Co., Amsterdam, pp. 3–137.

Parlange, J.-Y., 1980. Water transport in soils. Ann. Rev. Fluid Mech., 12: 77–102.

Parlange, J.-Y. and Starr, J.L., 1975. Linear dispersion in finite columns. Soil Sci. Soc. Am. Proc., 39: 817–819.

Parlange, J.-Y. and Starr, J.L., 1978. Dispersion in soil columns: Effect of boundary conditions and irreversible reactions. Soil Sci. Soc. Am. J., 42: 15–18.

Peaceman, D.W., 1977. Fundamentals of Numerical Reservoir Simulation. Elsevier, Amsterdam, 176 pp.

Rao, B.K. and Hathaway, D.L., 1989. Three-dimensional mixing cell solute transport model and its application. Ground Water, 27(4): 509–516.

Richards, L.A., 1931. Capillary conduction of liquids through porous mediums. Physics, 1: 318–333.

Schulz, H.D. and Reardon, E.J., 1983. A combined mixing cell/analytical model to describe

two-dimensional reactive solute transport for unidirectional groundwater flow. Water Resour. Res., 19(2): 493–502.

Schweich, D. and Sardin, M., 1981. Adsorption, partition, ion exchange and chemical reaction in batch reactors or in columns. J. Hydrol., 50: 1–33.

Schweich, D., Sardin, M. and Gaudet, J.P., 1983. Measurement of a cation exchange isotherm from elution curves obtained in a soil column: Preliminary results. Soil Sci. Soc. Am. J., 47(1): 32–37.

Sposito, G., 1989. The Chemistry of Soils. Oxford University Press, New York, N.Y., 277 pp.

van Genuchten, M.Th. and Alves, W.J., 1982. Analytical solutions of the one-dimensional convective–dispersive solute transport equation. U.S. Dep. Agric., Tech. Bull. No. 1661, 151 pp.

Van Ommen, H.C., 1985. The "mixing-cell" concept applied to transport of non-reactive and reactive components in soils and groundwater. J. Hydrol., 78: 201–213.

Yortsos, Y.C., 1987. The relationship between immiscible and miscible displacement in porous media. A.I.Ch.E. (Am. Inst. Chem. Eng.) J., 33: 1912–1915.